Qeios

An approach to robust fatigue life prediction to be used in early design stages

Peter Cronemyr* and Robert Eriksson[+]

** Senior Associate Professor, Logistics and Quality Management, Department of Management and Engineering, Linköping University, Sweden, peter.cronemyr@liu.se*

[+] Senior Associate Professor, Solid Mechanics, Department of Management and Engineering, Linköping University, Sweden, robert.eriksson@liu.se

Abstract. Many engineering structures eventually fail through fatigue. Design against fatigue is one of the more important parts of the engineering design process in order to avoid injuries/fatalities, improve sustainability and decrease costs. Design against fatigue is often a complicated and time-consuming process. New, faster, and sufficiently accurate engineering tools are much needed to allow for quick computational estimates as well as robust and risk-minimized engineering solutions. By combining knowledge from the fields of solid mechanics and quality management, such a tool has been developed and is proposed in this paper. By combining easy-to-use tools for robust design and probability design with engineering tools for stress analysis and fatigue analysis, regression equations and response surfaces can be developed to be used for choosing a robust solution. Hence reducing the sensitivity to variation in loads, material characteristics and other noise factors. After a design has been selected, a more detailed analysis can be carried out to validate the solution. Preliminary results from an application of analysis and design of an airplane wheel axle are presented.

Keywords: Fatigue life assessment, Robust Design, Probabilistic Design, Early Design Stages

Statements and Declarations

The research presented in this paper was funded by Linköping University through the project SEED 2021. There are no financial or non-financial interests that are directly or indirectly related to the work carried out for this paper.

https://doi.org/10.32388/BG6QWB

1. Introduction

As an introduction, the problem of integrating advanced fatigue analysis into the early stages of the design process is briefly addressed. It is followed by outlining the purpose of the paper, which is to present and propose a tool, that may help solving the problem.

1.1 The problem – Fatigue analysis too late in the design process

Most engineering structures eventually fail through fatigue where gradual damage accumulation in a material leads to complete failure with load cycles. Design against fatigue has become one of the more important parts of the engineering design process in order to avoid injuries/fatalities, improve sustainability and decrease costs (Gustafsson, 2012; Segersäll, 2014; Kahlin, 2017). However, since fatigue analysis is complicated and time-consuming, there is a tendency to conduct fatigue analysis late, or last, in the design process – only validating designs already optimised for other criteria such as cost, weight, or manufacturability, taking maximum allowed stress levels into account. Hence, fatigue analysis is not part of a robust solution which may lead to a product with high sensibility to variability of noise factors such as usage, material, and environmental factors (Cronemyr, 1999; Cronemyr, 2000).

Probabilistics have been incorporated in fatigue analyses in various ways. Most frequently, probabilistics is used in planning and evaluation of fatigue tests yielding S-N curves and fatigue limits for design (Foucherau *et al.*, 2014; Pyttel *et al.*, 2016; Bai *et al.*, 2017; D'Angelo and Nussbaumer, 2017; Hoole *et al.*, 2019) often by the use of Monte Carlo simulations (Foucherau *et al.*, 2014; Bai *et al.*, 2017; D'Angelo and Nussbaumer, 2017). Furthermore, various probabilistic methods are used to allow for design curve calibration with limited experimental data (Dias *et al.*, 2019; Klawonn, 2020; Klawonn and Beck, 2020a; Li *et al.*, 2020).

Other common topics for probabilistic approaches are handling the influence of material defect distributions and the influence of surface roughness on fatigue (Koutiri *et al.*, 2013; Pineau and Antolovich, 2016; Abroug *et al.*, 2018; Fomin *et al.*, 2018; Ai *et al.*, 2019; Szmytka *et al.*, 2020; El Khoukhi *et al.*, 2021) as well as the influence of notches, stress gradients and component size (Musinski and McDowell, 2012; Sadek and Olsson, 2014; Ai et al, 2019; Klawonn and Beck, 2020b; Liu *et al.*, 2020). For all of these topics, a common approach is the use of a weakest link concept (Koutiri *et al.*, 2013; Sadek and Olsson, 2014; Abroug *et al.*, 2018; Liu *et al.*, 2020).

Probabilistics is also used to account for variable amplitude loading (Karlen and Olsson, 2012; Kocanda and Jasztal, 2012; Sun *et al.*, 2014; Baptista *et al.*, 2017; Leonetti *et al.*, 2020) either by establishing probabilistic S-N curves trough Monte Carlo simulations (Baptista *et al.*, 2017) or by the use of an equivalent stress amplitude (Karlen and Olsson, 2012).

The aforementioned studies are largely concerned with variability in material properties and various size effects (including influence of notch root radius). More seldom do one encounter studies that accounts for uncertainties in applied load or performs optimization of component geometry with respect to fatigue. Previous structural optimization efforts tend to focus on worst case loading scenarios.

Johannesson *et al.* (2009) argue that enhanced VMEA (Variation Mode and Effect Analysis, see also Chakhunashvili (2006)) should be used in early design stages and based on the results of these, the most critical components causing the most variation could be identified. However, enhanced VMEA may be too complicated for everyday engineering activities. This is also in line with what Svensson (2004) argues; that methods for improving fatigue reliability in industry should not primarily consist of more complex models but should rather concentrate on reducing scatter and uncertainty. Svensson and Johannesson (2013) comply with that and propose

that the traditional concept of using safety factors is too rigid and that probabilistic methods are usually absent in fatigue problems.

New, faster, and *sufficiently accurate* engineering tools for robust fatigue engineering are much needed to allow for quick computational estimates in early design stages leading to robust and risk-minimized engineering solutions. Commercial CAE software packages are available that provide functions for multidisciplinary optimisation, some of them even with fatigue analysis, but those found by the authors do not facilitate robust and probabilistic design activities connected to advanced fatigue analysis.

1.2 The purpose of the paper – a tool for fatigue engineering in early design stages

The purpose of this paper is to propose such a tool. It has been developed by combining previously well-established techniques and knowledge from the fields of Solid Mechanics and Quality Management. For robust design and probability design, easy-to-use tools like Excel and Minitab have been used. They were, on the other hand, combined with advanced structural analysis tools, in our case Ansys, for finite element based stress analyses. Regression equations and response surfaces have been developed, to be used for choosing a robust solution, and hence reducing the sensitivity to variation in loads, material characteristics and other environmental noise factors. After a design has been proposed and selected by using the tool in an early stage of the design process, a more detailed fatigue analysis can be carried out to validate the solution later in the design process. To illustrate the tool, preliminary results from an application of analysis and design of an airplane wheel axle are presented.

2. Methodology

The two methodologies, one from the fields of Solid Mechanics and one from Quality Management, that have been combined in the proposed tool are described below: Fatigue analysis and Robust design. Furthermore, the model and design/noise factors used for the application example are described.

2.1 Fatigue analysis

Fatigue life predictions frequently act as a go/no go criterion for structural designs. Figure 1 illustrates the position of the fatigue analysis in a typical design process. Design processes may of course vary between different industries, but it is not unusual that the fatigue analysis occurs relatively late in a large and complex design process. This despite that unsatisfactory results in the fatigue analysis can cause another full design iteration.

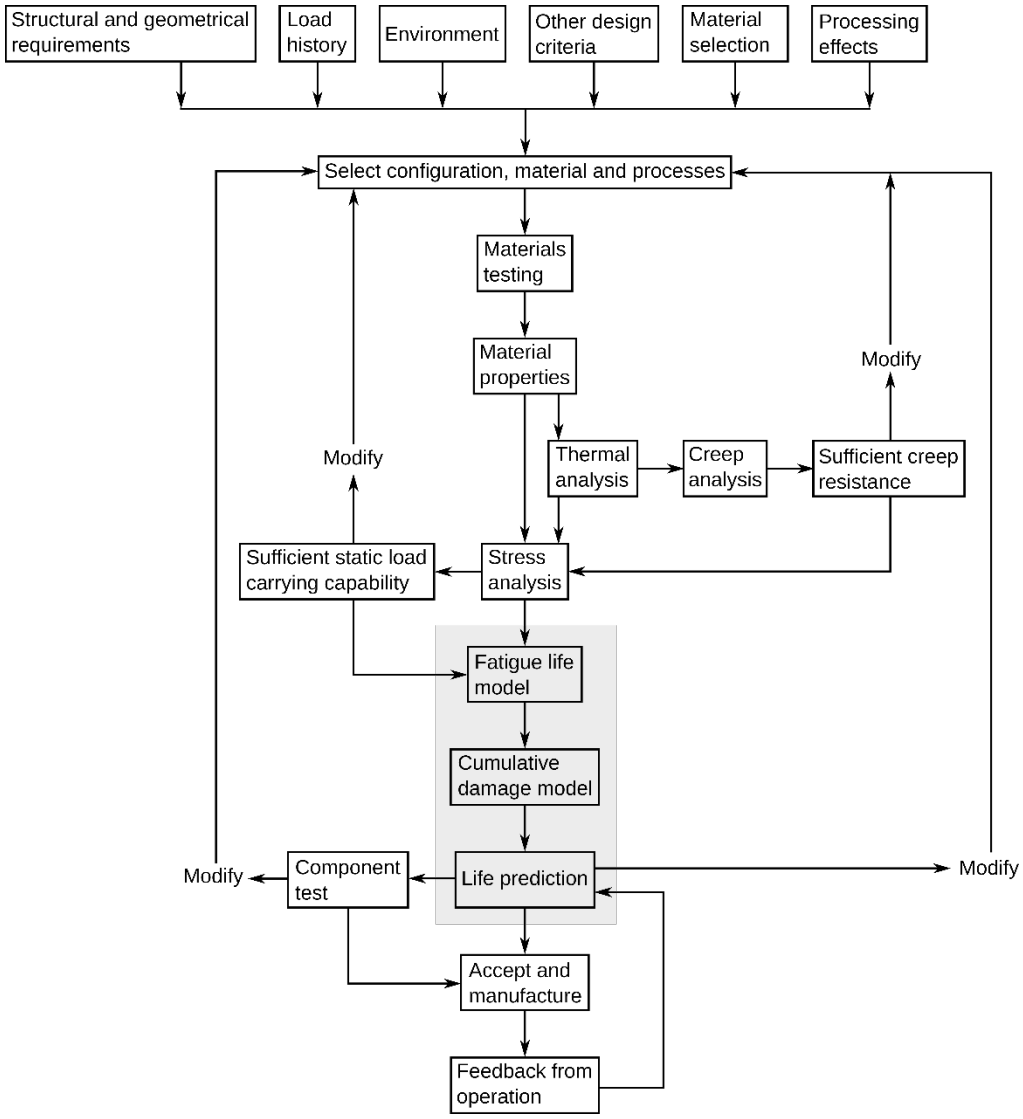

Figure 1. Fatigue analysis in the design process, loosely based on Stephens *et al.* (2001).

2.2 Robust design methodology

Robust Design Methodology (RDM) aims to making a product's or a process' performance predictable, i.e. insensitive to variation of uncontrollable noise factors (Phadke, 1989; Bergman and Klefsjö, 2010; Montgomery, 2013). These can be anything from the weather or material properties to how customers use the product. On the other hand, what could be controlled in the design process are the design factors, e.g. geometrical properties of a product. A general model for a product or a process with controllable design factors and uncontrollable noise factors is given in Figure 2.

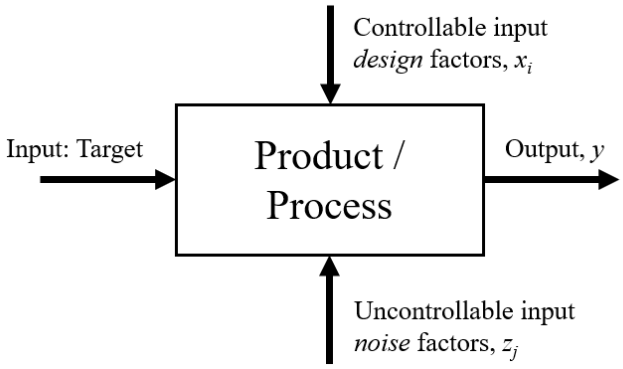

Figure 2. A general model for a product or a process with design and noise factors (Phadke, 1989)

Hence the performance of a product or process can be expressed as $y = f(x_i, z_j)$. In order to have a predictable performance y, one should eliminate (or at least reduce) the influence of the noise factors z_j by controlling the design factors x_i. How could it be done?

RDM was introduced by, among others, Genichi Taguchi already in the 1950s (Bergman and Klefsjö, 2010). The main purpose was to design, i.e. set up, experiments with design factors and noise factors (normally uncontrollable but controllable in the experiments) using a setup called orthogonal arrays (Phadke, 1989). There is however another, easier to understand, method called Design of Experiments (DoE) (Bergman and Klefsjö, 2010; Montgomery, 2013) which is the method we use in this paper. The main objective of the experiments is to detect how design factors and noise factors influence the product's performance, both one-at-a-time and how they influence the performance by factor interactions, something that can be difficult to detect in so-called changing-one-factor-at-a-time experiments (Bergman and Klefsjö, 2010; Montgomery, 2013).

By setting (at least) one low and one high level of each factor and then designing experiments with combinations of both levels of all factors we get a so-called full factorial design (Bergman and Klefsjö, 2010; Montgomery, 2013). In Figure 3 a DoE is given with two levels (– and +) of three factors (A, B, C), hence $2^3 = 8$ experiments. If there were five factors A, B, C, D, and E, a full factorial design would include $2^5 = 32$ experiments.

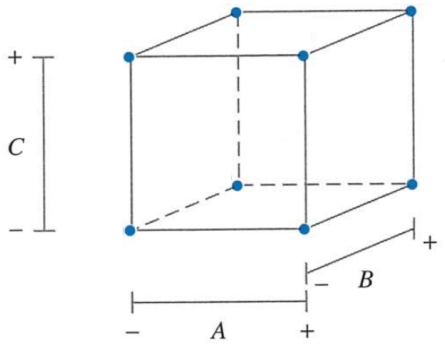

A	B	C	Y
–	–	–	y_1
+	–	–	y_2
–	+	–	y_3
+	+	–	y_4
–	–	+	y_5
+	–	+	y_6
–	+	+	y_7
+	+	+	y_8

Figure 3. DoE with a 2^3 factorial design 0

Notice that the factors A, B, and C can be either design factors x or noise factors z at some low and high levels. The outputs y_i are given by the results from the actual experiments, which could be carried out as real-life or laboratory experiments, surveys, or simulations using some advanced calculation tool. By analysing the outputs y_i we can determine which factors and interactions that are significant (Bergman and Klefsjö, 2010; Montgomery, 2013). The model is linear and bilinear but without curvature, i.e. no higher order terms. That may not be good enough for detailed analysis but is good enough for choosing a good design (see more explanations below). In Figure 4 results from two factorial experiments are presented. In the left example there is no interaction between A and B. In the right example there is an interaction. In the right case, if A is a design factor and B is a noise factor, then there is a specific value of A (between – and +) that will cancel out any influence from variations in B. That is basically what is called a *robust design*, which will minimise variation of the output and make the response predictable. Another type of robust design not described further here, is to take advantage of the response's curvature.

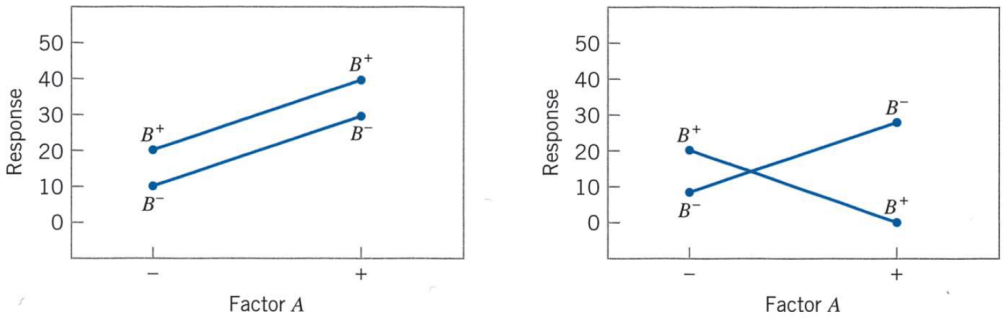

Figure 4. Factorial experiments, without (left), and with (right) interaction between factors A and B (Montgomery, 2013)

Significant factors and interactions can be used to set up a regression equation calculating fitted values $\bar{y}$ and residuals $y–\bar{y}$. If the residuals are low, i.e. coefficient of determination R^2 is close to 100 %, the regression equation $\bar{y}$ can be used as an approximation of y (Bergman and Klefsjö, 2010; Montgomery, 2013). The general expression for $\bar{y}$ with *one* design factor x and *one* noise factor z is: $\bar{y} = a + b\,x + c\,z + d\,xz$, where a, b, c, and d are constants (Bergman and Klefsjö, 2010; Montgomery, 2013). In that case the *robust design* is given by setting: $x = – c/d$, which will eliminate the influence of z and give the predictable (constant) output: $\bar{y} = a – bc/d$. With *more than one* design factor and *more than one* noise factor, the robust design is an equation of the design factors. The regression equation $\bar{y}$ can be visualised as a response surface, see Figure 5.

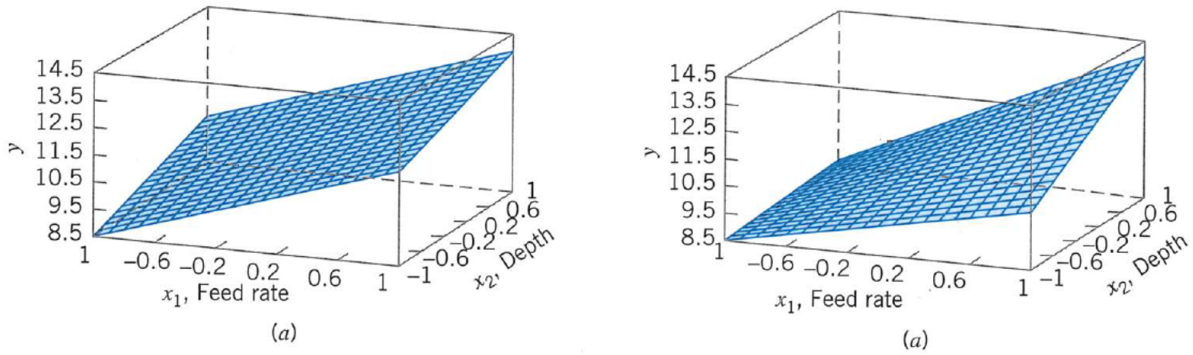

Figure 5. Response surfaces. Left: without factor interaction. Right: with factor interaction (Montgomery, 2013)

A response surface without interactions is linear, while a response surface with interactions is bilinear. Furthermore the response surface may have a curvature, i.e. include higher-order terms such as quadratic terms, but none of the examples given in Figure 5 does. However, if the real response y has a curvature, the regression $\bar{y}$ will only give correct results in the corners. That is why sometimes a midpoint, where all factors have a mid-value between – and +, is added to the DoE setup. The residual $y–\bar{y}$ in the midpoint is then divided in half and added (or subtracted) as a constant to the regression equation. It is still linear or bilinear, without curvature, but it is better than the original regression. Remember that the regression equation is *sufficiently accurate*, only to be used when selecting a robust and risk-minimized engineering design. Even so, *in case of curvature*, the regression equation should not – or should very cautiously – be extrapolated outside of the low and high boundaries of the DoE.

The regression $\bar{y}$ can then be used as a simulation tool for different probability distributions of the design factors x and noise factors z, so-called Probability Design. In Figure 6, a simple example of a Monte Carlo Simulation, as often used in Probability Design, is given for a static stress problem (not fatigue). In each one of 10,000 simulation runs, a random value sampled from the *expected* Load distribution has been subtracted from a random value sampled from the *measured* Strength distribution, hence giving a probability distribution of the Residual strength. This is known as the load/strength approach to reliability (Svensson and Johannesson, 2013). If the Residual strength is less than zero, the product will break. As can be seen, the probability of failure is 0.33%, which may be an acceptable risk. Otherwise, the means and/or distributions of Load and/or Strength must be altered, and new simulations of the Residual strength have to be carried out.

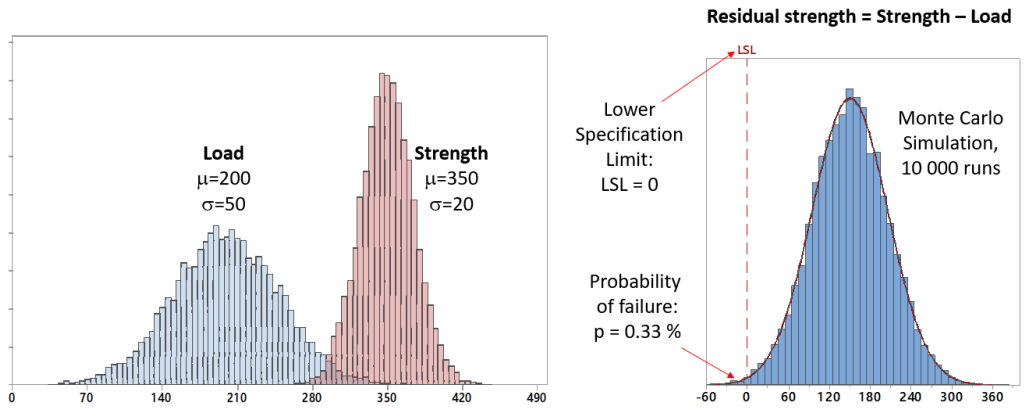

Figure 6. A Monte Carlo Simulation of Residual Static Strength, as used in Probability Design.

In the example above both factor distributions are normal (with mean μ and standard deviation σ), but factor distributions can have 'any' shape, e.g. normal, skewed, uniform, triangular, or some advanced shape derived from measurements. Because of the central limit theorem, the result variable is often normally distributed. By altering the values of the design factors and/or modifying the means and/or distributions of the noise factors, hopefully, a robust design can be achieved with acceptable and predictable performance.

2.3 The used model and design/noise factors

In order to have a reasonably realistic example, an example component was chosen loosely based on the fatigue case study by Le May (2010) which involved fatigue fracture in a Cessna L19 Bird Dog aircraft wheel axis. The axis finally ruptured during a rough landing. The case study revealed a fatigue crack that had obviously existed for some time and had grown from taxiing in rough terrain. The fracture surface also showed periods of crack arrest attributed to overloads from previous rough landings. The component is shown in Figure 7 and the point of crack initiation has been marked; it is located at the notch radius at the base of the axis.

Some dimensions of the component, such as the outer diameter of the wheel axis and the plate attaching to the landing gear, were considered to be determined by the surrounding design and unsuitable to change. Two geometrical dimensions were considered to be possible to vary without any changes in the remaining design: the inner diameter of the wheel axis, D, and the radius of the shoulder fillet, R; both are defined in Figure 7. The parameters D and R are hence taken as design factors. Chosen values were D=19 mm (D low) or D=29 mm (D high) and R=1 mm (R low) or R=2 mm (R high).

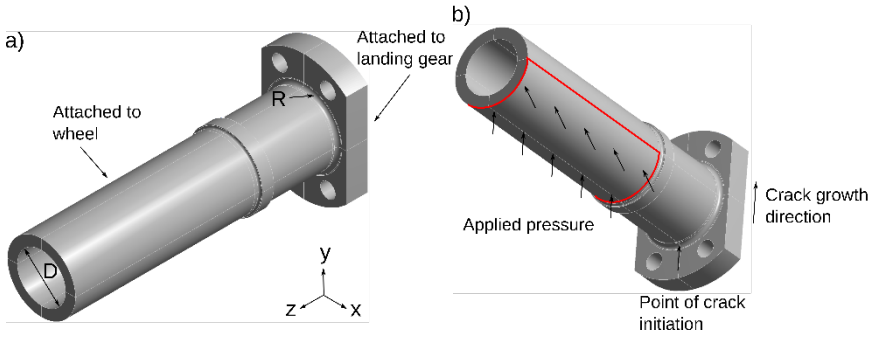

Figure 7. The studied component: a Cessna wheel axis. a) Definition of geometrical parameters. b) Point of crack initiation and crack growth direction.

The material of the component and the load spectrum are unknown to the authors and some assumptions and simplifications had to be done. A simple load spectrum was chosen, shown in Figure 8, which consists of:

1. Taxiing in the terrain prior to any rough landing. The mean stress, σ_{m1}, is determined entirely by the weight of the airplane and the stress amplitude, σ_{a1}, depends on the terrain. The number of cycles spent in this phase is n_1.
2. Landing causing an overload with mean stress σ_{m2} and stress amplitude σ_{a2}. The number of landings is n_2. Depending on the size of the maximum load, $\sigma_{max} = \sigma_{m2} + \sigma_{a2}$, the material may or may not plasticise.
3. Taxiing in the terrain after the landing. The mean stress, σ_{m3}, is now determined by the weight of the airplane as well as any residual stresses introduced due to plasticity. The stress amplitude, σ_{a3}, depends on the terrain and the number of cycles spent in this phase is n_3.

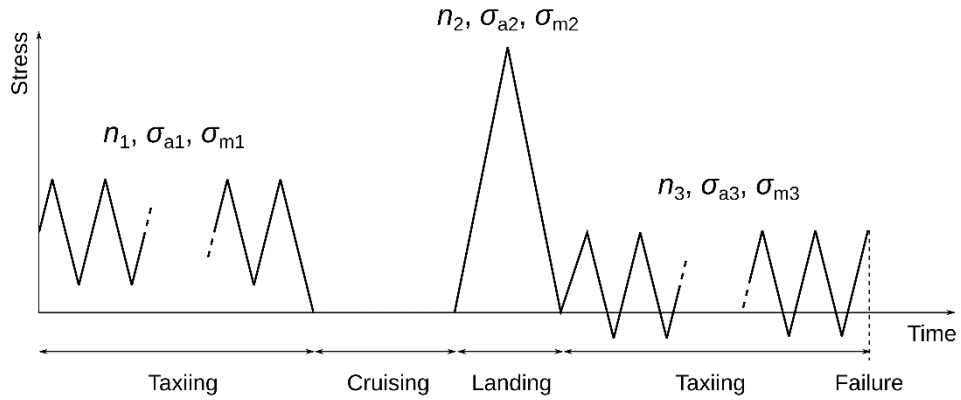

Figure 8. Simplified wheel axis load spectrum used in this study.

A stress-based fatigue model of the type

$$\sigma_i^0 = S_f N_i^b \text{ for } i = 1, 2, 3 \qquad \text{(eq. 1)}$$

was used where σ_i^0 is the stress amplitude at zero mean stress for the ith phase in the load spectrum, N_i is the corresponding number of cycles to failure and S_f and b are material parameters. A Goodman mean stress correction was performed, i.e.

$$\sigma_{ai} = \sigma_i^0 \left(1 - \frac{\sigma_{mi}}{\sigma_{UTS}}\right) \text{ for } i = 1, 2, 3 \qquad \text{(eq. 2)}$$

where σ_{ai} is the ith stress amplitude at the corresponding mean stress σ_{mi} giving the same life as σ_i^0. Hence

$$\sigma_{ai} = \left(1 - \frac{\sigma_{mi}}{\sigma_{UTS}}\right) S_f N_i^b \text{ for } i = 1, 2, 3 \qquad \text{(eq. 3)}$$

The number of cycles spent in phase 1, n_1, was arbitrarily set to 10 000 cycles and only one rough landing was assumed, giving $n_2 = 1$ cycle. The remaining fatigue life was consequently spent in n_3 and linear damage accumulation was assumed in order to get n_3 (i.e. Palmgren-Miner's rule). Failure was assumed to occur when the accumulated damaged reached 1, hence giving

$$\frac{n_1}{N_1} + \frac{n_2}{N_2} + \frac{n_3}{N_3} = 1 \Rightarrow n_3 = N_3 \left(1 - \frac{n_1}{N_1} - \frac{n_2}{N_2}\right) = N_3 \left(1 - \frac{10^4}{N_1} - \frac{1}{N_2}\right) \qquad \text{(eq. 4)}$$

The stresses σ_{ai} and σ_{mi} were taken as the z-component at the surface of the component at the location of crack initiation, as marked by arrows in Figure 7 b); the local stress at the fillet was use, thereby including notch effects. It should be noted that load sequence effects could be (at least roughly) accounted for by taking failure to occur at an accumulated damage other than 1; however, for simplicity, no such load sequence correction is made here.

The material of the wheel axis is not stated in Le May (2010) but is here taken to be a medium-carbon steel JIS S35C. Fatigue data for steel JIS S35C was taken from Databook on fatigue strength of metallic materials Vol. 1 (1996); the SN-curve is shown in Figure 9. Fitting eq. 1 to the data in Figure 9 yielded $b = -0.0768$. Under the assumption of constant b, minimum and maximum curves were introduced so that they enclosed all data points giving **Sf** = 641 MPa and **Sf** = 721 MPa for the minimum and maximum curves respectively, see Figure 9

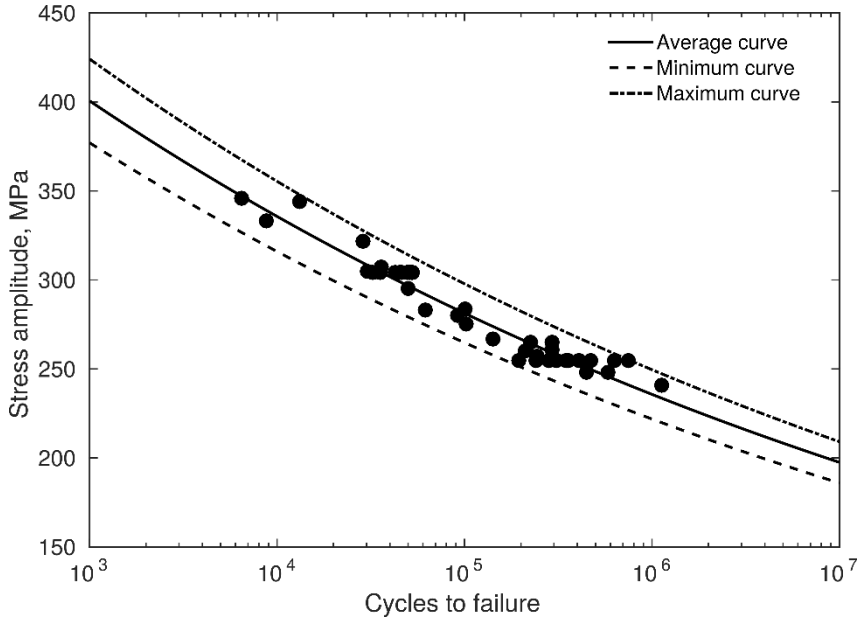

Figure 9. SN-curve for steel JIS S35C, taken from:
Databook on fatigue strength of metallic materials Vol. 1 (1996)

Stresses at the shoulder fillet was modelled using the commercial finite element code Ansys Workbench 17.2. The material was modelled as elasto-plastic with linear kinematic hardening using the material data given in Table 1. The yield limit, σ_y, and the ultimate tensile strength, σ_{UTS}, were taken from Databook on fatigue strength of metallic materials Vol. 1 (1996); the Young's modulus, E, and the Poisson's ratio, ν, were set to values common for steels and the tangent modulus, H, was assumed to be a hundredth of the Young's modulus.

E, GPa	ν	σ_y, MPa	σ_{UTS}, MPa	H, GPa
200	0.3	373	612	2

Table 1. Material parameters used for the structural analysis.

The inner surfaces of the four screw holes had all their degrees of freedoms fixed and the applied load was applied as a pressure on the lower half of the wheel axis, as illustrated in Figure 7. The pressure was calculated from estimated loads (in N) divided by the projected area of the wheel axis (0.004428 m^2). The loads were estimated in the following way:

- Prior to the rough landing, the applied mean load, **M1**, was taken as half the approximate weight of a Cessna giving **M1** = 4.5 kN. The applied load amplitude, **A1**, prior to the rough landing was taken as a fraction of half the weight of the Cessna giving **A1** = 1.35 kN (**A1** low) for taxiing in smooth terrain and **A1** = 2.7 kN (A1 high) for taxiing in rough terrain (corresponding to 0.3 and 0.6 times the half-weight).
- During the landing, the applied load amplitude, **A2**, was taken as **A2** = 3.6 kN (**A2** low) for a smooth landing and **A2** = 7.2 kN (**A2** high) for a rough landing (corresponding to 0.8 and 1.8 times the half weigh of the Cessna). The mean load, **M2**, during landing was **M2** = **A2**, i.e. the max load during the landing was taken as 2*__A2__.
- After the landing, during taxiing, **A1** and **M1** were applied just as prior to the landing.

After completed FE analysis, z-component of the stress was extracted at the crack initiation point (illustrated in Figure 7). A mesh convergence analysis was performed to ensure stable results.

3. Results from the Analysis

We first present the results from the structural analysis, followed by the results from the DoE and the robust design analyses. Lastly, the 'best' design is chosen in different ways using different criteria.

3.1 Results from the structural analysis

Figure 10 shows the equivalent plastic strain after the rough landing for the case where **D** = 29 mm and **R** = 2 mm. Figure 10 a) shows that **A2** = 3.6 kN did not cause plastic deformation whereas **A2** = 7.2 kN did, as seen in Figure 10 b). The influence of plasticity on the maximum stresses is illustrated in Figure 11 which compares maximum stress, σ_{max}, prior to and after the landing for the same geometry. As evident from Figure 11 , maximum stress remains the same after the landing for the case of **A2** = 3.6 kN, as seen in Figure 11 a) and b). For **A2** = 7.2 kN, the plasticity introduced during landing causes the mean stress to drop giving lower maximum stress after the landing, as seen in Figure 11c) and d). This is more clearly seen in Figure 12 where the mean stress can be seen to drop for all cases that result in plastic deformation during the landing.

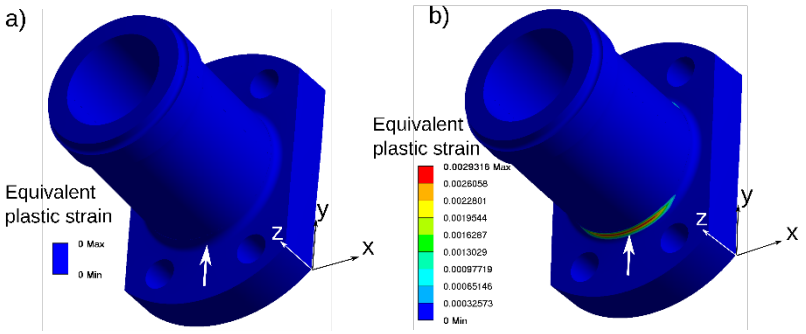

Figure 10. **D** high, **R** high, arrow marks crack initiation point: a) **A1** low, **A2** low, after landing; b) **A1** low, **A2** high, after landing.

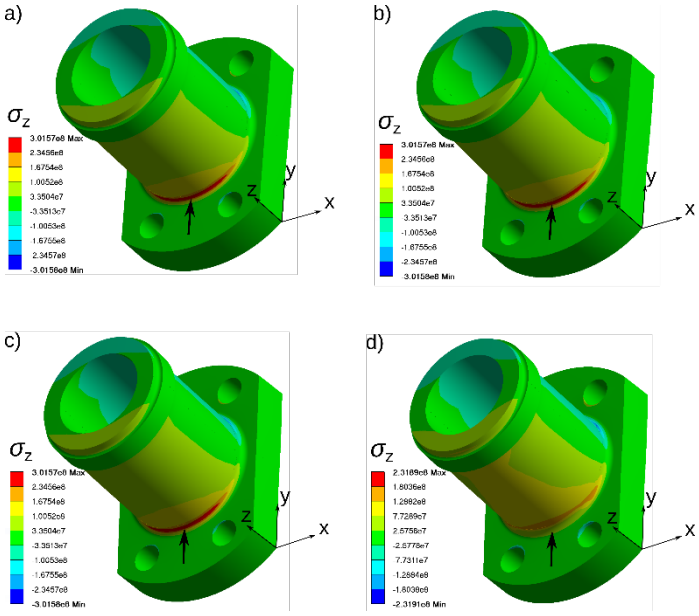

Figure 11. **D** high, **R** high, arrows mark crack initiation point: a) **A1** low, **A2** low, σ_{max} prior to rough landing; b) **A1** low, **A2** low, σ_{max} after rough landing; c) **A1** low, **A2** high, σ_{max} prior to rough landing; d) **A1** low, **A2** high, σ_{max} after rough landing.

The resulting z-component stress amplitudes at the fillet (i.e. at the point of expected crack initiation) are shown in Figure 12 for all combinations of **A1** and **A2** at **R**=2 mm and **D**=29 mm. It is clear that the overload at high **A2**

gave rise to plasticity and caused further fatigue load to occur at a lower mean load. The fillet mean stress and stress amplitude was extracted and used for life assessments as previously described.

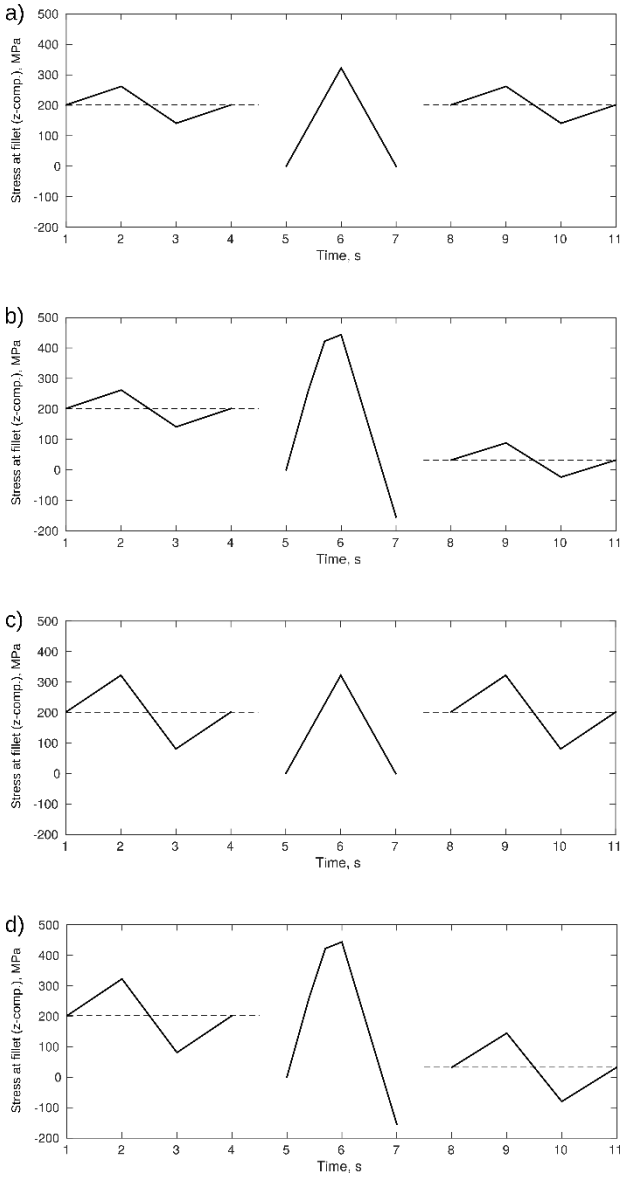

Figure 12. The stress amplitude in the z-direction at the fillet radius (**D** high, **R** high): a) **A1** low, **A2** low, no plasticity; b) **A1** low, **A2** high, plasticity during landing lowers mean stress; c) **A1** high, **A2** low, no plasticity; d) **A1** high, **A2** high, plasticity during landing lowers mean.

3.2 DoE setup and life calculation results

The model that was used in the test, as described above, contained the factors as given in Table 2.

Factor	Type	Name	low	high
x_1	Design	**D** [mm]	19	29
x_2	Design	**R** [mm]	1	2
z_1	Noise NORM(2025;340)	**A1** [N]	1350	2700
z_2	Noise NORM(5400;900)	**A2** [N]	3600	7200
z_3	Noise NORM(681;20)	**Sf** [MPa]	641	721
Y	Result	**Life** [cycles]	*From life calculation*	
Log(Y)	Result	**Log(Life)**	*10-Logarithmic life*	

Table 2. DoE factors

According to Johannesson *et al.* 0, there are several types of scatter and uncertainty that should be considered when conducting fatigue life assessments, *e.g.* scatter in strength of materials and geometry, model uncertainty and load uncertainty. The model in our case contained two design factors; **D** and **R**, and three noise factors; **A1**, **A2**, and **Sf**. The low and high values to be used in the DoE were set to typical low and high values as follow. The values of **A1** corresponded to typical amplitudes for 'smooth runway' and 'bumpy runway'. The values of **A2** corresponded to amplitudes for 'soft landing' (without material plasticizing, according to calculations) and 'hard landing' (with material plasticizing, according to calculations). The values of **Sf** corresponded to typical low and high values from material data. In our case, a factor *per se* for the model uncertainty (*e.g.* the plasticity model) was not included. However, since a very advanced computational model of the plasticity behaviour was used, the model uncertainty is reduced.

The noise factors' probability distributions used later in the life probability simulations, where set to be normally distributed with an average μ and a standard deviation σ so that μ+/–2σ corresponded to the high and low values, i.e. 95 % of variation falls between the low and the high values, while 2.5 % fall above high and 2.5 % below low.

The expected life (in cycles) was calculated for all $2^5 = 32$ experiments. The specification limit, i.e. the minimum acceptable life, was set to 10^9 cycles (assuming a fatigue limit of 10^8 cycles) and was used in the evaluation of the designs in the life probability simulations. Since life, **Y**, has a very skewed distribution 0, the 10-logarithmic of the life, **Log(Y)**, was used as the result factor in the DoE and the life probability simulations. Histograms and normal probability plots of **Y** and **Log(Y)** are given in Figure 13. If all points fall between the red lines the distribution is normal, otherwise skewed. As can be seen, and due to the central limit theorem (Johannesson *et al.*, 2009), **Log(Y)**, is fairly normal.

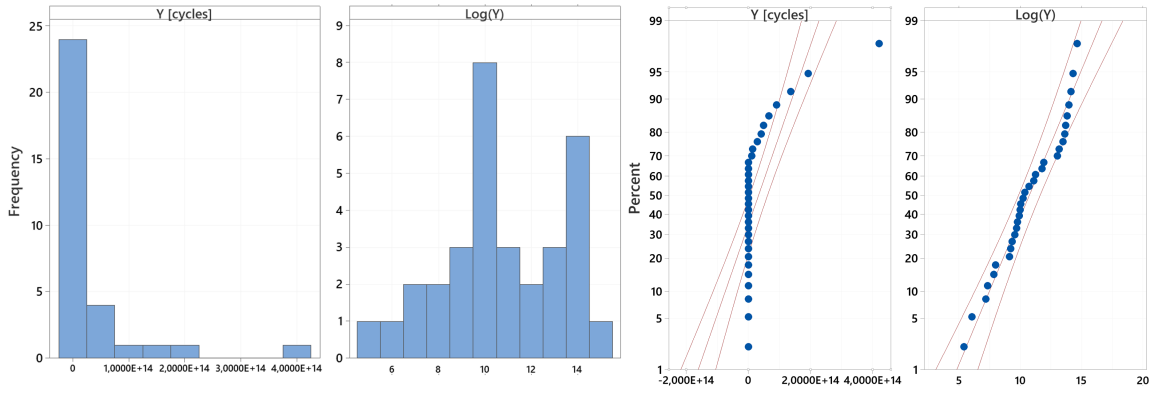

Figure 13. Histograms and normal probability plots of **Y** (skewed) and **Log(Y)** (normal)

The complete DoE setup and life calculation results are given in Table 3.

#	D [mm]	R [mm]	A1 [N]	A2 [N]	Sf [MPa]	Life Y	Log(Y)
1	19	1	1350	3600	641	1.75E+11	11.24
2	29	1	1350	3600	641	2.07E+09	9.32
3	19	2	1350	3600	641	1.06E+13	13.03
4	29	2	1350	3600	641	1.24E+11	11.09
5	19	1	2700	3600	641	2.10E+07	7.32
6	29	1	2700	3600	641	2.49E+05	5.40
7	19	2	2700	3600	641	1.27E+09	9.11
8	29	2	2700	3600	641	1.49E+07	7.17
9	19	1	1350	7200	641	4.16E+13	13.62
10	29	1	1350	7200	641	1.42E+13	13.15
11	19	2	1350	7200	641	9.09E+13	13.96
12	29	2	1350	7200	641	2.93E+13	13.47
13	19	1	2700	7200	641	5.00E+09	9.70
14	29	1	2700	7200	641	1.64E+09	9.21
15	19	2	2700	7200	641	1.09E+10	10.04
16	29	2	2700	7200	641	3.53E+09	9.55
17	19	1	1350	3600	721	8.07E+11	11.91
18	29	1	1350	3600	721	9.59E+09	9.98
19	19	2	1350	3600	721	4.90E+13	13.69
20	29	2	1350	3600	721	5.72E+11	11.76
21	19	1	2700	3600	721	9.71E+07	7.99
22	29	1	2700	3600	721	1.15E+06	6.06
23	19	2	2700	3600	721	5.89E+09	9.77
24	29	2	2700	3600	721	6.88E+07	7.84
25	19	1	1350	7200	721	1.93E+14	14.28
26	29	1	1350	7200	721	6.59E+13	13.82
27	19	2	1350	7200	721	4.20E+14	14.62
28	29	2	1350	7200	721	1.36E+14	14.13
29	19	1	2700	7200	721	2.32E+10	10.36
30	29	1	2700	7200	721	7.85E+09	9.89
31	19	2	2700	7200	721	5.05E+10	10.70
32	29	2	2700	7200	721	1.63E+10	10.21

Table 3. Complete DoE setup and life calculation results

3.3 DoE Results

By defining and analysing the DoE the regression equation from the 32 experiments can be derived (we used Minitab but it can be done using standard equations for regression analysis). Only including significant factors, i.e. factors with a contribution greater than due to random variation 00, the following regression equation is derived.

$$\textbf{Log(Y)} = 10.6329 - 0.337657*\textbf{D} + 3.22912*\textbf{R} - 0.002905*\textbf{A1} + 0.000300*\textbf{A2} + 0.008329*\textbf{Sf} + 0.000040*\textbf{D}*\textbf{A2} - 0.000403*\textbf{R}*\textbf{A2} \quad \text{(eq. 5)}$$

The significant factors are: one constant term, four linear factors, and two bilinear factors. *No more interactions of grade two or higher were significant.* By using the regression equation, fitted values $\bar{y}$ for **Log(Y)** as well as the

coefficient of determination R^2 can be calculated. In this case R^2 = 99.9 % which is very high, i.e. the regression equation gives very accurate values, albeit in the points of the DoE setup. However, as mentioned above, there may be a curvature of the response surface. Hence an extra life calculation has been carried out in the midpoint, i.e. in a point where the design and noise factors have their mid values, see Table 4 below.

#	D [mm]	R [mm]	A1 [N]	A2 [N]	Sf [MPa]	Life Y	Log(Y)
33	24	1.5	2025	5400	681	1.45E+10	10.16

Table 4. DoE midpoint and life calculation results

1.1

Using the regression equation in the midpoint gives $\bar{y}$ = 10.70, which is 5% higher than the calculated **Log(Y)** 10.16. As described above, the constant term in the regression equation may be modified to:

10.6329 – (10.70 – 10.16) / 2 = 10,3629. However, the change is very small. Furthermore, since different designs will be compared to one another, the constant is of no importance.

So, the conclusion so far is that the curvature is weak, meaning higher order terms are not needed, and therefore we can use the regression equation to evaluate the robustness of different designs.

3.4 Robust solution

The linear factors in the regression are called main effects in DoE, while the bilinear factors are called interactions. They can be seen in Figure 14.

First, in the main effects plots, the slopes can be seen. Some are positive and some are negative. The greatest linear effect comes from **A1**, with considerably higher life expectancy for 'smooth runway' than 'bumpy runway', which is expected. Also, looking at **A2**, a 'hard landing' (with material plasticizing) will increase the life expectancy, also as expected. Variation of **Sf** has a very small influence.

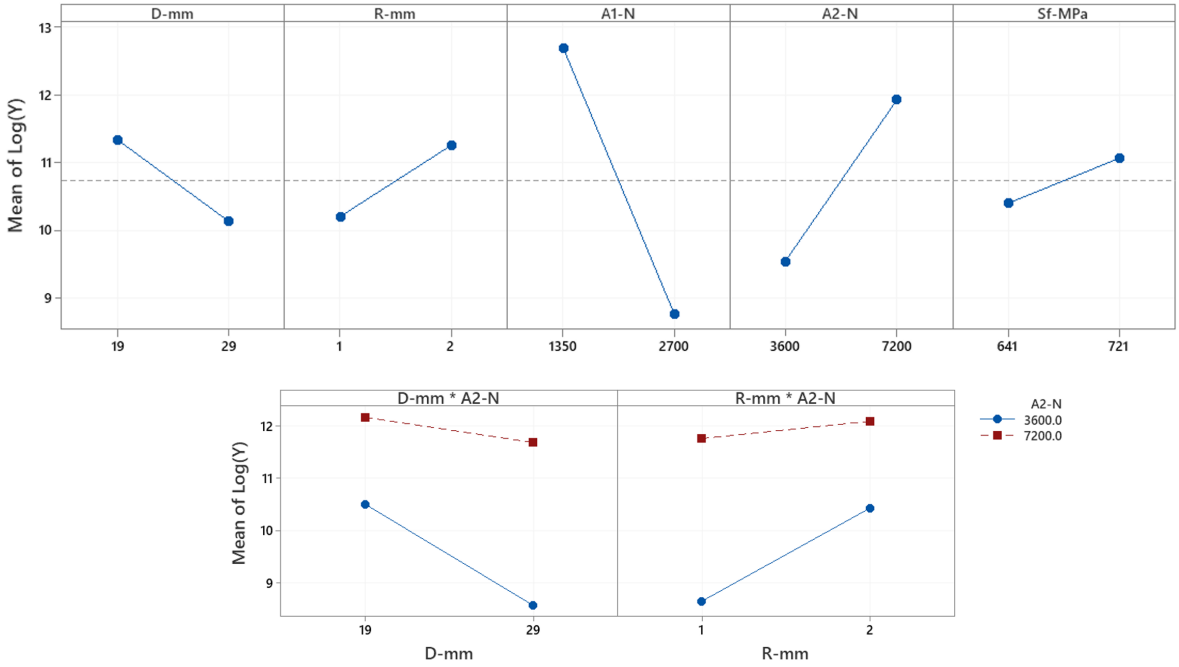

Figure 14. Main effects plots and Interaction plots of **Log(Y)**

Second, the interaction plots in Figure 14 show the interactions between design factors **D** and **R** with the noise factor **A2**. There are no significant interactions between the design factors and **A1** or **Sf**. It would have been feasible if there were interactions between **D** and/or **R** and **A1**, since **A1** is the noise factor with the highest influence. In such a case, by choosing specific values of **D** and/or **R**, the **A1** influence could have been cancelled out, but unfortunately that is not the case.

As seen in the interaction plots in Figure 14 the lines do not cross in either plot, but they would if the **D** range were extended to less than **D** = 19 mm and if the **R** range were extended to more than **R** = 2 mm. The solution for a robust design given above ($x = -c/d$) is only valid when there is an interaction between one design factor and one noise factor. In the current regression equation, there are interactions between two design factors and one noise factor. Hence, the robust solution, which minimises the influence from **A2**, derived from the regression equation is: **R** = 0.74 + 0.10***D**. So, if **D** is 19 mm, then the robust solution is given by **R** = 2.6 mm, i.e. more than 2, or if **R** is 2 mm, then the robust solution is given by **D** = 13 mm, i.e. less than 19.

Extrapolating the regression equation could be risky, so additional life calculations were carried out in four points combining the new values of **D** and **R**. Using the regression equation in the additional points give $\bar{y}$ values that deviate somewhat from the calculated **Log(Y)** values. The regression equation gives deviations of max 5 % from calculated life and an R^2 = 98,6 %. Since this is meant to be a *sufficiently accurate* design tool, we are confident using this regression equation also in the points outside the original design.

3.5 Choosing the best design

By using the regression equation with set values of the design factors and random values of the noise factors, life expectancy distributions can be simulated. We decided to make simulations for **D** = 13, 19 and 29 mm, combined with **R** = 1, 2 and 2.6 mm, i.e. nine different designs. The noise distributions for **A1**, **A2** and **Sf** used are given in Table 2.

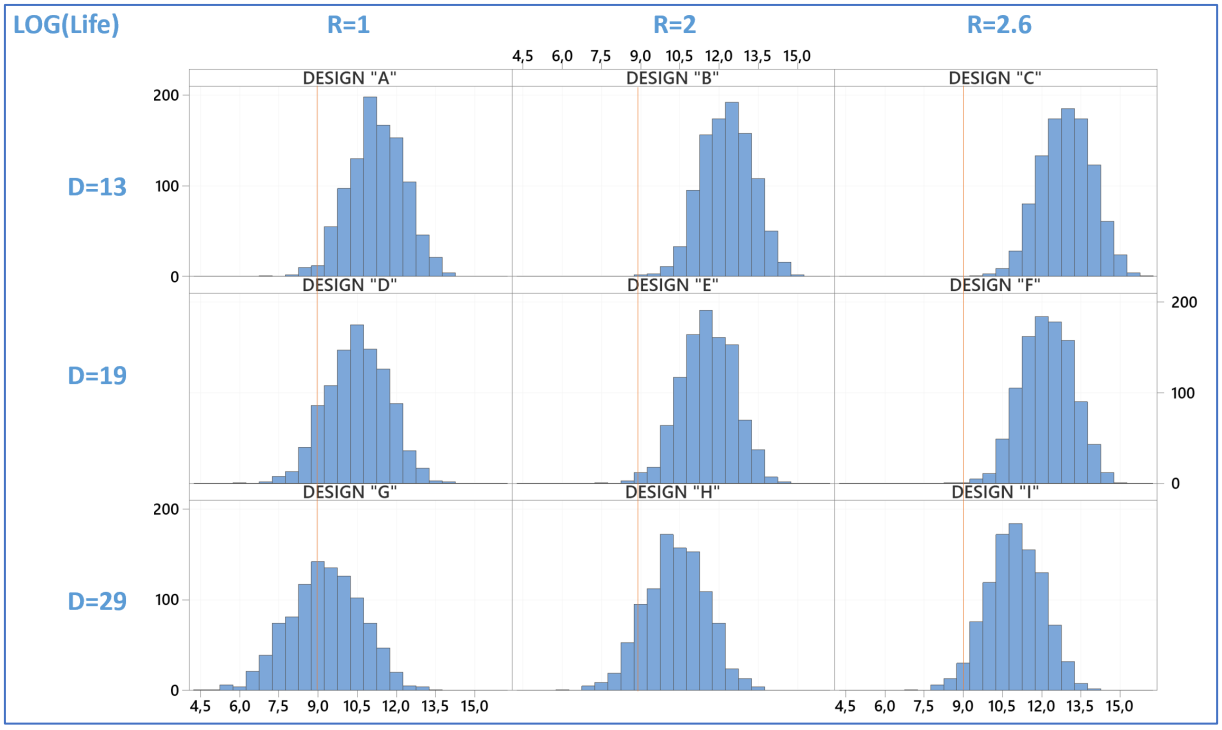

Figure 15. Monte Carlo simulations (10,000 runs) of life **Log(Y)** distributions for nine different designs

In Figure 15 the life distributions of the different designs are given. The red line is the specification limit, i.e. the minimum acceptable life, 10^9 cycles. The total area of each graph is 100% and the area to the left of the red line corresponds to the probability of a life < 10^9 cycles for each specific design. The results are also presented in Table 5.

DESIGN	Mean	St Dev	Min	Max	p [%]
"A" D=13 R=1	11.239	1.055	7.165	14.163	2.0
"B" D=13 R=2	12.296	**0.976**^{c}	8.792	15.167	0.1
"C" D=13 R=2.6	**12.931**^{a}	0.993	**9.730**^{b}	15.940	**0.0**^{d}
"D" D=19 R=1	10.506	1.156	6.093	13.787	10.0
"E" D=19 R=2	11.564	1.008	7.720	14.296	0.5
"F" D=19 R=2.6	12.198	**0.976**^{c}	8.696	15.069	0.1
"G" D=29 R=1	9.2856	1.386	4.306	13.310	41.7
"H" D=29 R=2	10.343	1.155	5.933	13.619	12.2
"I" D=29 R=2.6	10.977	1.053	6.910	13.894	2.5

Table 5. Results from Monte Carlo simulations of life **Log(Y)**. p = (probability of life < 10^9) [%].
Note: The 'best' performances are indicated by bold text and scenario index.

From Table 5 the 'best' design can be selected. However, what does 'best' mean? Is it (*a*) the 'optimal' design with the highest mean life? Or (*b*) the best case looking at the 'worst-case scenario' with the highest minimum life value? Or (*c*) the 'robust' design with the lowest variation of the expected life? Or (*d*) the 'safest' solution with the lowest probability of life < 10^9? From our experience, scenarios (*a*) and (*b*) are more commonly used when designing products than scenarios (*c*) and (*d*). Applying (*a*) is sometimes called Optimal Design, while (*b*) is called Conservative or Worst-Case Design, (*c*) is called Robust Design, and (*d*) is called Probability Design.

In our case, using either of scenarios (*a*), (*b*) or (*d*), we would select design "C" as the 'best' design with a probability of life < 10^9 less than 0.05 %. By choosing the most robust solution, scenario (*c*), we would go for design "B" or design "F".

However, if **D** = 13 mm and/or **R** = 2.6 mm is not an acceptable design, due to some other constraints, another solution can be chosen by using the results from the simulations and applying a scenario for the 'best' solution. Maybe if **D** must be at least 19 mm and **R** must be lower or equal to 2 mm (as in the original DoE setup), design "E" would be chosen instead. Then p = 0.5 %, may be too high of a risk for "failure" i.e., life < 10^9. Then the design factors have been set to **D** = 19 mm and **R** = 2 mm, so the distributions of the noise factors have to be altered. How could we restrict i.e., reduce, the variation of the noise factors?

By only using results from specific rows in the DoE setup, given in Table 3, new regression equations can be derived for specific values of the noise factors (regression equations not given here). We have made simulations for several scenarios; **A1** at low level: 'always smooth runway', **A1** at high level: 'always bumpy runway', **A2** at low level: 'always soft landing', and **A2** at high level: 'always *at least one* hard landing'. The **Sf** distribution was not altered.

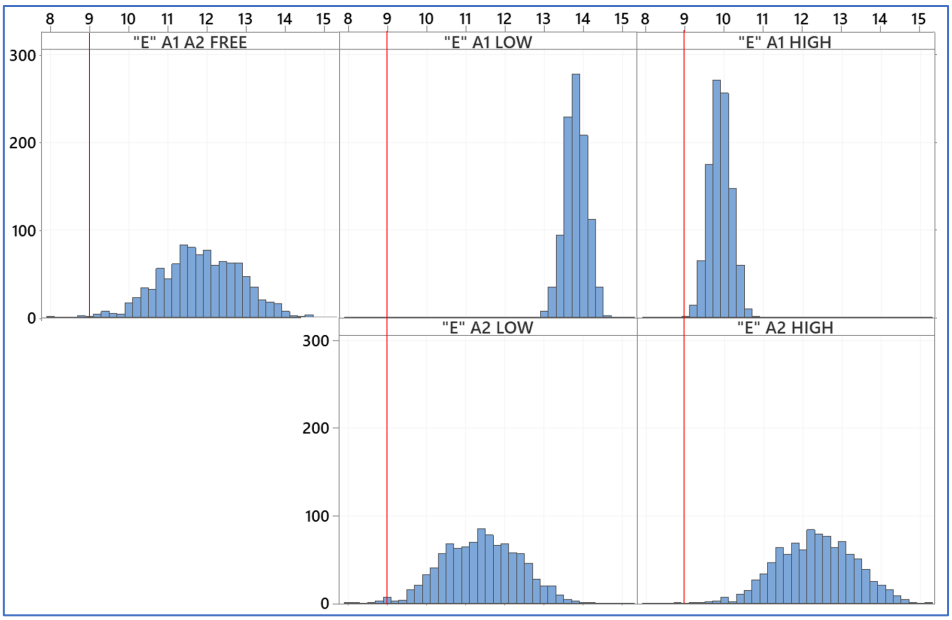

Figure 16. Monte Carlo simulations of life **Log(Y)** for design "E" with specific values on **A1** and **A2**

In Figure 16 and Table 6 the simulation results for the selected design "E", with **D** = 19 mm and **R** = 2 mm and specific values on **A1** and **A2** are given.

"E" D=19 R=2	Mean	St Dev	Min	Max	p [%]
A1 A2 free	11.564	1.008	7.720	14.296	0.5
A1 low	13.797	0.278	12.977	14.627	0.0
A1 high	9.886	0.279	9.060	10.720	0.0
A2 low	11.394	0.975	7.910	14.271	0.9
A2 high	12.326	0.976	8.839	15.205	0.1

Table 6. Results from simulations of life **Log(Y)** for design "E" with specific values on **A1** and **A2**.

By restricting take-offs and landings to be either 'always on soft runways' (**A1** low) or 'always on bumpy runways' (**A1** high), the probability of life $< 10^9$ is $p < 0.05$ %, which is very low i.e., good. 'Always on soft runways' may be a feasible restriction for some applications and hence, could be recommended. It is clearly the best solution. However, 'always on bumpy runways' is more uncertain, both how it would be applied, and it also has a much lower expected mean life, albeit with a very low standard deviation.

By restricting landings to always be soft (**A2** low) would neither increase the life nor reduce the risk compared to letting **A2** vary freely. However, by controlling **A2** to a high level, meaning 'always *at least one* hard landing', would reduce the risk to $p = 0.1$ %, compared to $p = 0.5$ %, for letting **A2** vary freely. This means that plasticisation will increase the expected life, even if landing on bumpy runways. However, since it is not recommended to instruct pilots to do a hard landing – it would be difficult to make an *exactly right* hard landing with the risk of a *too hard* landing leading to static failure – it would be better to conduct the plasticisation by means of shot peening.

Our robust and risk-minimised design therefore is: **D** = 19 mm and **R** = 2 mm and also performing shot peening on the critical location of the wheel axis.

After selecting the preliminary design, the detailed design of the wheel axis can now carry on with more advanced and accurate analyses on life etc., in the 'normal' way.

4. Discussion and Conclusions

We present our learnings from testing the new approach. We also discuss the alternative, traditional, way of designing products against fatigue. What are the pros and cons of the two approaches? Lastly, we summarise our conclusions.

4.1 Learnings and need for further development

The proposed methodology is an easy-to-use, fast, and *sufficiently accurate* engineering tool to be used in early design stages to develop robust and risk-minimized engineering solutions. It utilises advanced tools for structural analysis in a combination with less advanced tools for robust and probability design.

Some things we learned on the way are listed below.

- Design and noise factors have to be chosen before setting up the DoE design. Design factors with low/high values should be chosen wisely to cover the possible values of the design to be developed. If chosen too narrow, results may need to be extrapolated or complemented with additional calculations. If chosen too wide, the response surface of the results may be too curved so extra midpoints need to be added. We tested both these scenarios.
- Noise factors also need to be chosen. The distributions of which may be difficult to estimate. In our case we assumed normally distributed noise factors, since it seemed rational, with 95 % of distributions within low/high values. We also tested with some skewed distributions, which did not alter the final results considerably.
- Once the DoE set-up was defined with low/high values of five factors, the $2^5 = 32$ experiments, i.e. life calculations, were conducted fairly straight-on, taking approximately 35 hours of CPU time.
- In order to get a useful regression equation, with linear and bilinear terms, fairly normally distributed results are needed. In our case we calculated **Log(Y)**, which was normal, so we could use that instead. Another approach would be to add nonlinear, higher-order, terms which is more advanced and requires a bigger DoE design (i.e., with more points). We found **Log(Y)** to be easy to use and give easy-to-use design estimations.
- Finding a robust solution, where the influence from noise factors can be eliminated, is not always easy, and sometimes not possible. In our case, we found that the influence from the noise factor **A2** (soft/hard landing) could be reduced, but not eliminated, by choosing a design outside of the original DoE set-up with **R** and **D** related as: $\mathbf{R} = 0.74 + 0.10\mathbf{*D}$. Those values of **R** and **D** were not feasible so other values, 'as close as possible' were chosen.
- The approach of using Monte Carlo simulation with 10,000 runs of probability factor distributions was very simple and easy to use. By comparing life distributions and probability of life less than specification limit, the safest, i.e. 'best', design could be selected.

4.2 Alternatives

There are many ways of performing a conventional fatigue analysis. In its simplest form, though, fatigue analysis would be used as a go/no go criterion for designs already finalized with respect to e.g. function, weight, cost and manufacturability. Such an analysis may be performed in the following way:

- The geometry is already given by previous design considerations. Here, the 'nominal' geometry, **D**=24 mm and **R**=1.5 mm, is used (i.e. the geometry in between the high and low levels of **D** and **R** used throughout this work).
- A structural analysis is performed on 'typical' operation loads. Here, this corresponds to operation on smooth runways and soft landings (i.e. the loads are taken as **A1** low and **A2** low, which, in this case, do not give rise to any plastic deformation).
- In the case of high cycle fatigue, such structural analyses are most often performed as linear-elastic (this might even be necessary for complex geometries to obtain results in reasonable time).
- The fatigue limit is often utilized for the component type of interest here, i.e. the life should exceed at least some 10^8 cycles, i.e. **Log(Y)** > 8.
- In the presence of means stress, some mean stress theory is applied to ensure that the component does not fail under combined mean load and variable load. Here, Goodman's mean stress theory is used.
- Safety factors are calculated from calculated stresses and the Goodman diagram. If the safety factors are sufficiently high, uncertainties in applied load are considered to have been accounted for and the design gets a "go".

Performing the steps outlined above, yields the following results. A linear-elastic finite element analysis on the geometry with **D**=24 mm and **R**=1.5 mm and applied loads **A1**=1.35 kN and **A2**=3.6 kN results in the fillet stresses (z-component) given in Table 7.

	Taxiing	**Landing**	**Taxiing**
$\boldsymbol{\sigma_m}$**, MPa**	192.59	154.07	192.59
$\boldsymbol{\sigma_a}$**, MPa**	57.78	154.07	57.78

Table 7. Results from conventional fatigue analysis; fillet stresses, z-component.

The fatigue limit for the current material is $\sigma_{fl} = 238$ MPa 0 which, using Goodman's mean stress theory, gives the maximum allowed stress amplitude, σ_{ai}^{max} i=1, 2, 3, as

$$\sigma_{ai}^{max} = \sigma_{fl}\left(1 - \frac{\sigma_{mi}}{\sigma_{UTS}}\right) \text{ for i=1, 2, 3} \qquad \text{(eq. 6)}$$

from which the safety factor, F_i i=1, 2, 3, can be calculated (with respect to variability of the stress amplitude) as

$$F_i = \frac{\sigma_{ai}^{max}}{\sigma_{ai}} \text{ for i=1, 2, 3} \qquad \text{(eq. 7)}$$

giving $F_1 = F_3 = 2.8$ (for taxiing) and $F_2 = 1.2$ (for landing).

For taxiing, the safety factor is certainly high enough to account for uncertainties in load. For landings, the safety factor might be on the low side, but considering landing load cycles being less frequent than taxiing load cycles, the component design would probably get a "go" and go into manufacturing. Alternatively, a larger fillet radius would be prescribed, and another life assessment made (e.g. an increase to **R**=2 mm gives safety factors of 3.3 and 1.3 for taxiing and landing respectively). However, it should be noticed that these safety factors do not give any indication of the probability of failure. So, the level of 'safety' is unknown.

4.2 Conclusions

Even though design against fatigue is often an important part of the engineering design process – in order to avoid injuries/fatalities, improve sustainability and decrease costs – it is seldom carried out in the early design stages, due to a considerably complicated and time-consuming process.

In this paper we propose a new, *fast, and sufficiently accurate* engineering tool for fatigue engineering to be used in early design stages. Such a tool is much needed to allow for quick computational estimates as well as robust and risk-minimized engineering solutions. It has been developed by combining previously well-established techniques and knowledge from the fields of Solid Mechanics and Quality Management. For robust design and probability design, easy-to-use tools like Excel and Minitab have been used. They were, on the other hand, combined with advanced engineering tools, in our case Ansys, for stress analysis and fatigue analysis. Regression equations and response surfaces have been developed, to be used for choosing a robust solution, and hence reducing the sensitivity to variation in loads, material characteristics and other environmental noise factors. An example of using the tool has been presented in the paper. After a design has been proposed and selected by using the tool in an early stage of the design process, a more detailed fatigue analysis can be carried out to validate the solution later in the design process.

The advantages of using the proposed tool against the traditional way of designing products against fatigue have been discussed.

The major findings were

- By using the proposed tool fatigue analysis can be performed in the early design process instead of only as a go/no go criterion for structural designs relatively late in the design process.
- The tool can be used to suggest design factors (e.g. geometry) early but can also be used to suggest how significant noise factors could be manipulated or reduced when the product is used, hence reducing the probability of failures.
- Most aspects of component design and component usage is included in a known probability of failure as opposed to the much cruder use of ‘safety factors’.

References

Abroug F, Pessard E, Germain G, Morel F. (2018), A probabilistic approach to study the effect of machined surface states on HCF behavior of a AA7050 alloy. *Int J Fatigue* 2018;116;473-489.

Ai Y, Zhu SP, Liao D, Correia JAFO, Souto C, De Jesus AMP, Keshtegar B. (2019), Probabilistic modelling of fatigue life distribution and size effect of components with random defects. *Int J Fatigue* 2019;126;165-173.

Ai Y, Zhu SP, Liao D, Correia JAFO, De Jesus AMP, Keshtegar B. (2019), Probabilistic modelling of notch fatigue and size effect of components using highly stressed volume approach. *Int J Fatigue* 2019;127;110-119.

Bai X, Xie L, Zhang R, Guan R, Tong A, Bai E. (2017), Measurement and estimation of probabilistic fatigue limits using Monte-Carlo simulations. *Int J Fatigue* 2017;95;229-235.

Baptista C, Reis A, Nussbaumer A. (2017), Probabilistic S-N curves for constant and variable amplitude. *Int J Fatigue* 2017;101;312-327.

Bergman, B. and Klefsjö, B. (2010) *Quality from Customer Needs to Customer Satisfaction*. 3rd ed., Studentlitteratur, 2010.

Chakhunashvili, A. (2006) *Detecting, identifying, and managing sources of variation in production and product development.* PhD thesis. Department of Quality Sciences. Chalmers. Göteborg.

Cronemyr, P. (1999) *Hållfare* (in Swedish). Hållfasthetsläras 30-års jubileumskonferens, Linköpings universitet.

Cronemyr, P. (2000) *Towards a Learning Organization for Product Development*. Licentiate thesis, Linköpings universitet.

Gustafsson, D., (2012), *High temperature fatigue crack propagation behaviour of Inconel 718.* Doctoral dissertation, Linköpings universitet.

D'Angelo L, Nussbaumer A. (2017), Estimation of fatigue S-N curves of welded joints using advanced probabilistic approach. *Int J Fatigue* 2017;97;98-113.

Databook on fatigue strength of metallic materials Vol. 1. (1996). Amsterdam: Elsevier

Dias JP, Ekwaro-Osire S, Cunha Jr A, Dabetwar S, Nispel A, Alemayehu FM, Endeshaw HB. (2019), Parametric probabilistic approach for cumulative fatigue damage using double linear damage rule considering limited data. *Int J Fatigue* 2019;127;246-258.

El Khoukhi D, Morel F, Saintier N, Bellett D, Osmond P, Le VD. (2021), Probabilistic modelling of the size effect and scatter in High Cycle Fatigue using a Monte-Carlo approach: Role of the defect population in cast aluminium alloys. *Int J Fatigue* 2021;147;106177.

Fomin F, Horstmann M, Huber N, Kashaev N. (2018), Probabilistic fatigue-life assessment model for laser-welded Ti-6Al-4V butt joints in the high-cycle fatigue regime. *Int J Fatigue* 2018;116;22-35.

Fouchereau R, Celeux G, Pamphile P. (2014), Probabilistic modelling of S-N curves. *Int J Fatigue* 2014;68;217-223.

Hoole J, Sartor P, Booker J, Cooper J, Gogouvitis XV, Schmidt RK. (2019), Systematic statistical characterisation of stress-life datasets using 3-Parameter distributions. *Int J Fatigue* 2019;129;105216.

Johannesson, P., Svensson, T., Samuelsson, L., Bergman, B., and de Maré, J. (2009), Variation Mode and Effect Analysis: An Application to Fatigue Life Prediction. *Quality and Reliability Engineering International*, 25: 167-179.

Kahlin, M. (2017), *Fatigue performance of additive manufactured Ti6Al4V in aerospace applications*. Licentiate thesis, Linköpings universitet.

Karlen K, Olsson M. (2012), A probabilistic model for the entire HCF domain based on equivalent stress - Simulations and experiments. *Int J Fatigue* 2012;36;9-17.

Klawonn A, Hagenacker A, Beck T. (2020), A probabilistic Haigh diagram based on a weakest link approach. *Int J Fatigue* 2020;133;105419.

Klawonn A, Beck T. (2020), Efficient staircase testing of probabilistic Haigh diagrams. *Int J Fatigue* 2020;137;105627.

Klawonn A, Beck T. (2020), A probabilistic Haigh diagram for notched components considering notch root plasticity due to high mean stresses. *Int J Fatigue* 2020;140;105813.

Kocanda D, Jasztal M. (2012), Probabilistic predicting the fatigue crack growth under variable amplitude loading. *Int J Fatigue* 2012;39;68-74.

Koutiri I, Bellett D, Morel F, Pessard E. (2013), A probabilistic model for the high cycle fatigue behaviour of cast aluminium alloys subject to complex loads. *Int J Fatigue* 2013;47;137-147.

Le May, I. (2010), *Procedia Engineering 2*, 59-64, doi: 10.1016/j.proeng.2010.03.006

Leonetti D, Maljaars J, Snijder HH. (2020), Probabilistic fatigue resistance model for steel welded details under variable amplitude loading - Inference and uncertainty estimation. *Int J Fatigue* 2020;135;105515.

Li C, Wu S, Zhang J, Xie L, Zhang Y. (2020), Determination of the fatigue P-S-N curves - A critical review and improved backward statistical inference method. *Int J Fatigue* 2020;139;105789.

Liu X, Wang R, Hu D, Mao J. (2020), A calibrated weakest-link model for probabilistic assessment of LCF life considering notch size effects. *Int J Fatigue* 2020;137;105631.

Montgomery, D. C. (2013), *Statistical Quality Control: A modern Introduction*. 7th ed. Singapore: John Wiley & Sons.

Musinski WD, McDowell DL. (2012), Microstructure-sensitive probabilistic modelling of HCF crack initiation and early crack growth in Ni-base superalloy IN100 notched components. *Int J Fatigue* 2012;37;41-53.

Phadke, M. (1989): *Quality Engineering using Robust Design*. Prentice Hall PTR, Englewood Cliffs, New Jersey.

Pineau A, Antolovich SD. (2016), Probabilistic approaches to fatigue with special emphasis on initiation from inclusions. *Int J Fatigue* 2016;93;422-434.

Pyttel B, Canteli AF, Ripoll AA. (2016), Comparison of different statistical models for description of fatigue including very high cycle fatigue. *Int J Fatigue* 2016;93;435-442.

Sadek S, Olsson M. (2014), New models for prediction of high cycle fatigue failure based on highly loaded regions. *Int J Fatigue* 2014;66;101-110.

Segersäll, M., (2014), *On thermomechanical fatigue of single-crystal superalloys.* Doctoral dissertation, Linköpings universitet.

Stephens RI, Fatemi A, Stephens RR, HO Fuchs. (2001), Metal fatigue in engineering. John Wiley & Sons, New York. 2001

Sun Q, Dui HN, Fan XL. (2014), A statistically consistent fatigue damage model based on Miner's rule. *Int J Fatigue* 2014;69;16-21.

Svensson, T. (2004) Model complexity versus scatter in fatigue. Invited article. *Fatigue & Fracture of Engineering Materials & Structures* 27, 981-990.

Svensson, T. and Johannesson, P. (2013) Reliable fatigue design, by rigid rules, by magic or by enlightened engineering. *Procedia Engineering*, 66 (2013) 12-25.

Szmytka F, Charkaluk E, Constantinescu A, Osmond P. (2020), Probabilistic Low Cycle Fatigue criterion for nodular cast-irons. *Int J Fatigue* 2020;139;105701.